Electronic Supplementary Information (ESI)

One-dimensional zirconium-doped titanate nanostructures for rapid and selective removal of multiple heavy metal ions from water

Chen Zou[a], Xiaojuan Zhao[a] and Yan Xu*[a]

[a] *State Key Lab of Inorganic Synthesis and Preparative Chemistry, Jilin University, 2699 Qianjin Street, Changchun 130012, China. E-mail: yanxu@jlu.edu.cn.*

Metal ion adsorption by ion-exchange.

For comparison, the pseudo-first-order kinetic model was used to analyze the absorption kinetic data as follows:[1]

$$\ln(q_e - q_t) = \ln q_e - K_1 t$$

where K_1 is the pseudo-first-order kinetic constant.

For comparison, the absorption data were also analyzed using the Freundlich isotherm

$$q_e = K_F C_e^n$$

model as follows:[2]

where K_F and n are the Freundlich constants.

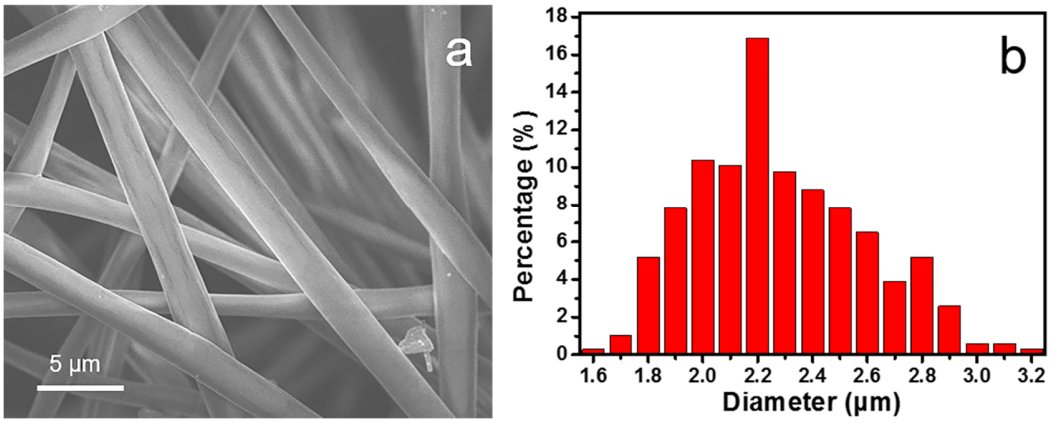

Figure S1. Characterizing the as-spun fibers. (a) SEM images. (b) Diameter distributions.

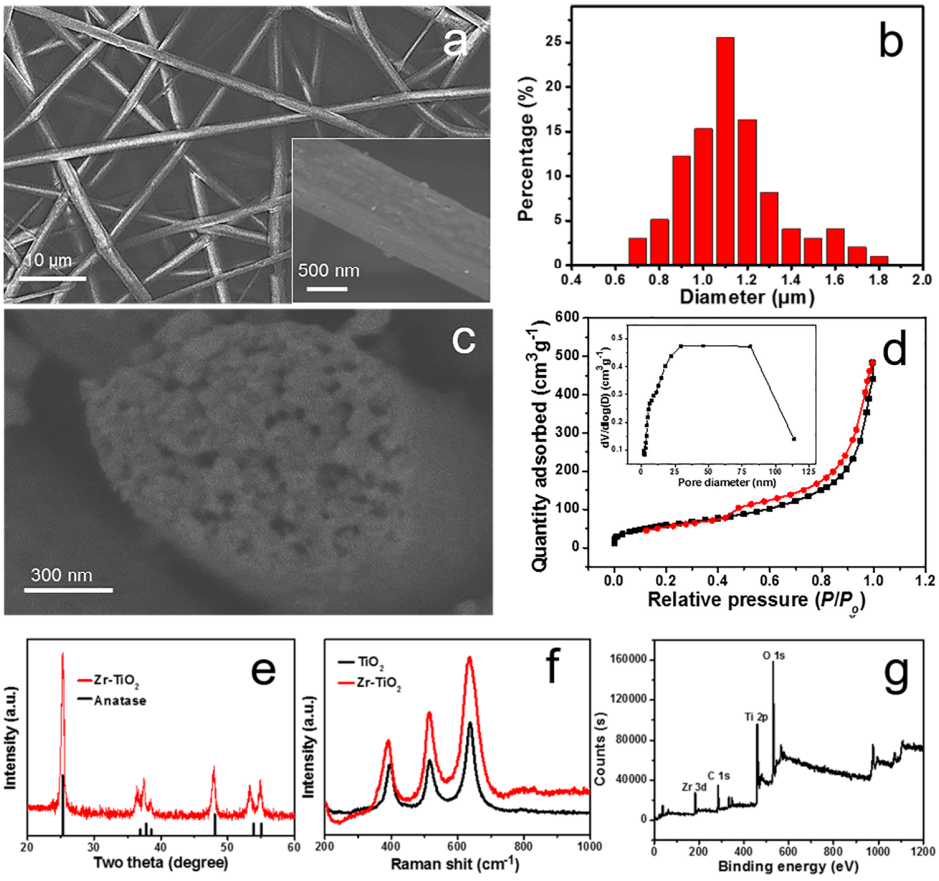

Figure S2. Characterizing the Zr-TiO_2 precursor fibers. (a) SEM showing uniform thickness. Inset showing uneven surface. (b) Diameter distributions. (c) High-magnification SEM showing nanopores. (d) N_2 sorption isotherm. Inset showing the BJH pore size distribution. (e) XRD showing pure anatase phase. (f) Raman spectrum. (g) XPS survey spectrum.

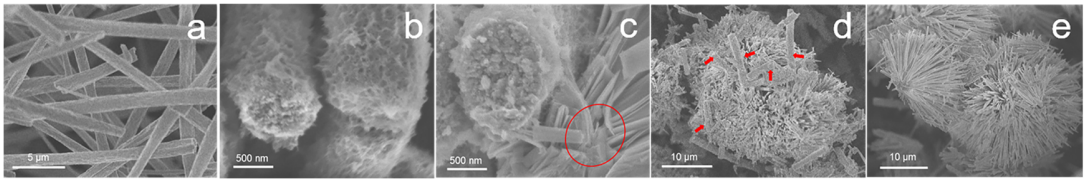

Figure S3. Mesostructural transformation during the hydrothermal reactions. (a) 0h. (b) 3h. (c) 9h. (d) 12h. (e) 24h.

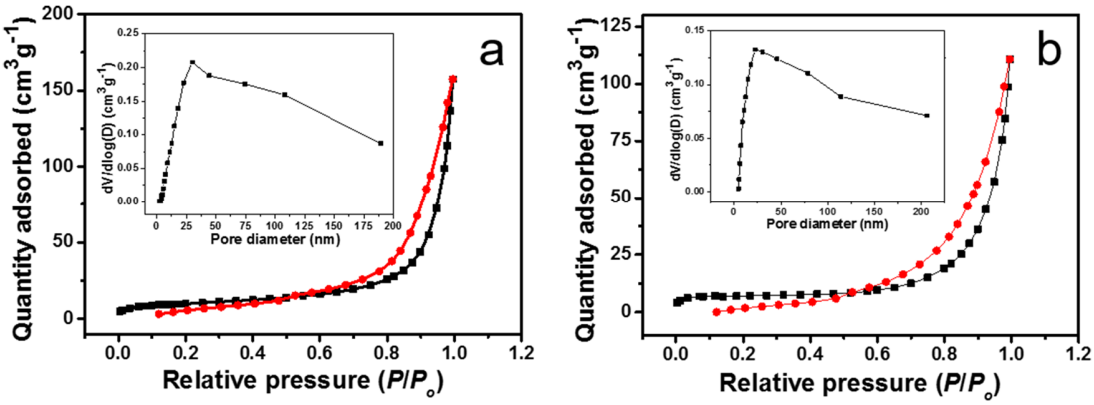

Figure S4. Characterizing the textural properties using N_2 sorption isotherm. Inset showing the BJH pore size distribution. (a) ZTNT2. (b) ZTNT3.

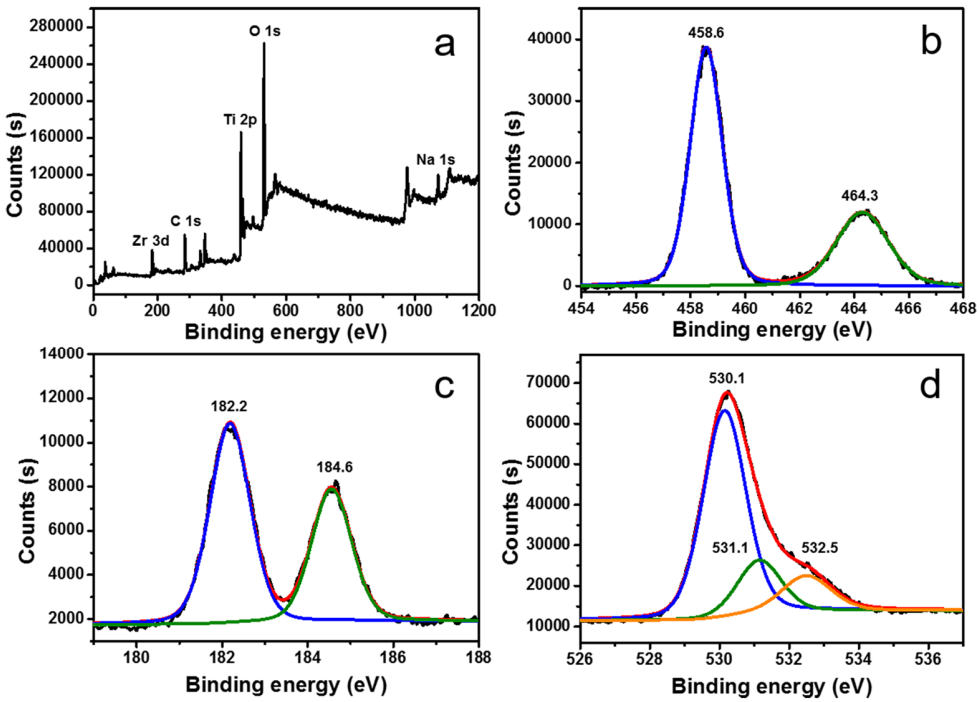

Figure S5. XPS spectra of ZTNT1. (a) Survey spectrum. (b) Deconvoluted peaks of Ti 2p. (c) Deconvoluted peaks of Zr 3d. (d) Deconvoluted peaks of O 1s.

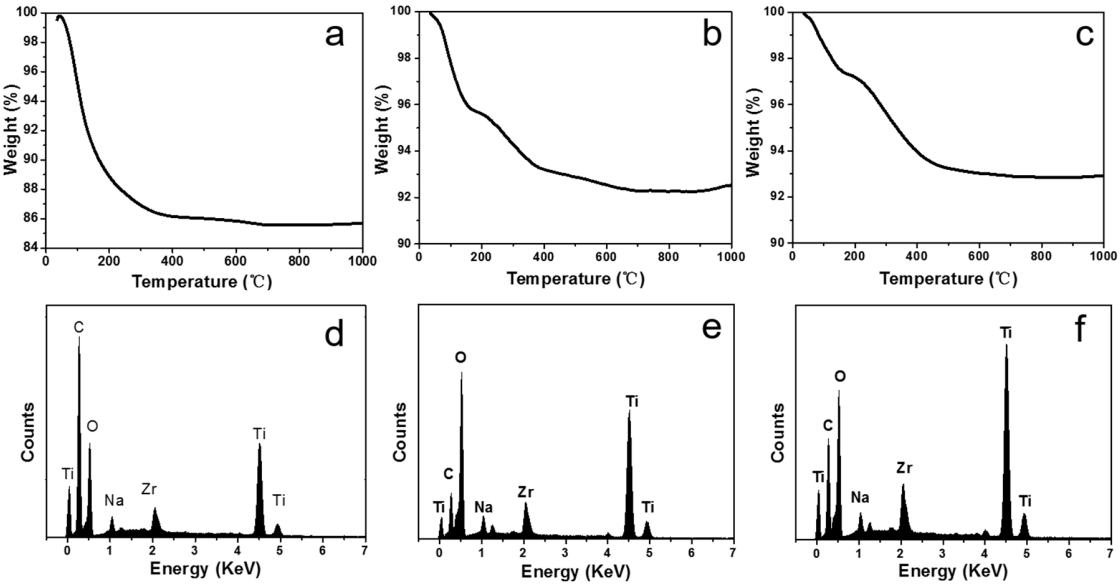

Figure S6. Thermogravimetric analysis of (a) ZTNT1, (b) ZTNT2 and (c) ZTNT3. EDS analysis of (d) ZTNT1, (e) ZTNT2 and (f) ZTNT3.

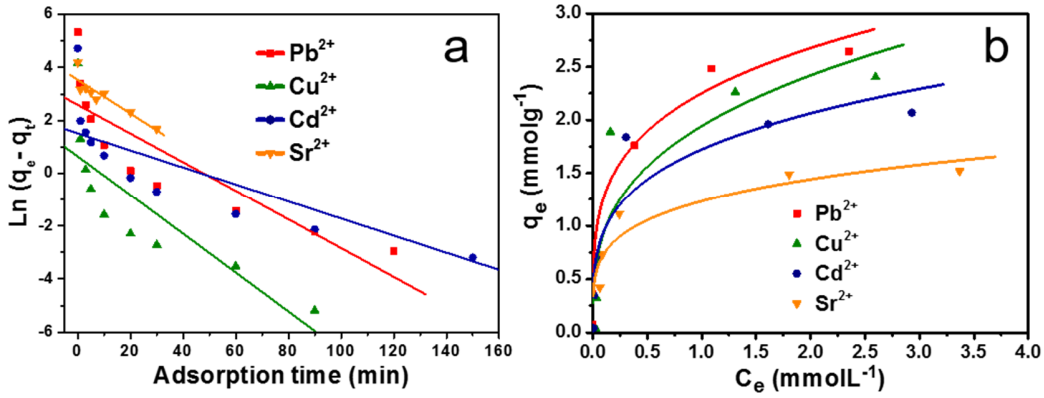

Figure S7. Fitting the adsorption data of ZTNT1 using (a) the pseudo-first-order adsorption kinetic model and (b) the Freundlich adsorption isotherm model.

Table S1. Adsorption Parameters of ZTNT1

Adsorbents	Adsorbates	Freundlich isotherm model			Pseudo-first-order kinetic model	
		K_F ($mmolg^{-1}$)	n	R^2	K_1 (min^{-1})	R^2
ZTNT1	Pb^{2+}	2.25	0.25	0.9529	0.054	0.7305
	Cu^{2+}	1.94	0.32	0.7298	0.073	0.6301
	Cd^{2+}	1.72	0.26	0.8205	0.032	0.7358
	Sr^{2+}	1.23	0.23	0.8217	0.063	0.7925

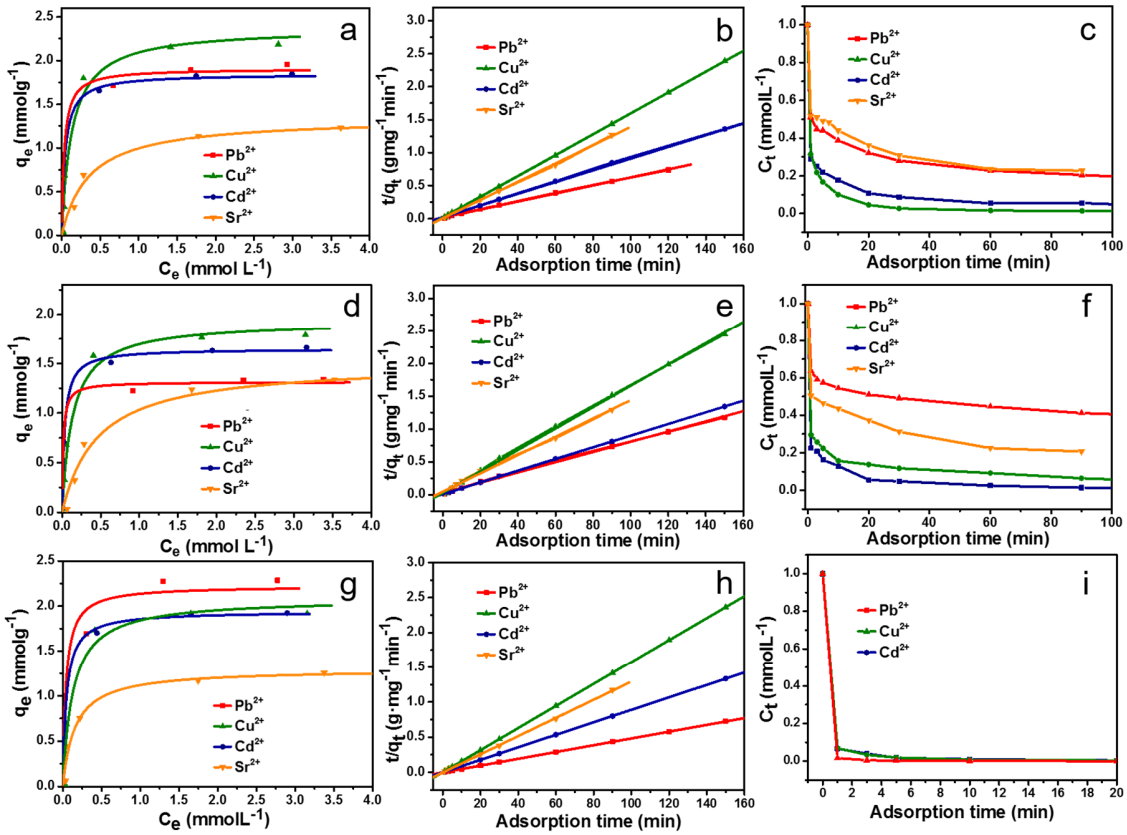

Figure S8. Characterizing the adsorption properties of ZTNT2 (a-c), ZTNT3 (d-f) and TNT (g-i) for M^{n+}: (a,d,g) Langmuir adsorption isotherm model. (b,e,h) The pseudo-second-order adsorption kinetic model. (c,f,i) Adsorption kinetic curves.

Table S2. Adsorption Parameters of ZTNT2 and ZTNT3

Adsorbents	Adsorbates	Langmuir isotherm model			Freundlich isotherm model			*Pseudo* second-order kinetic model		*Pseudo* first-order kinetic model	
		q_{max} ($mmolg^{-1}$)	K_L	R^2	K_F ($mmolg^{-1}$)	n	R^2	K_2 ($gmg^{-1}min^{-1}$)	R^2	K_1 (min^{-1})	R^2
ZTNT2	Pb^{2+}	1.91	29.61	0.9912	1.63	0.24	0.9469	0.003	0.9991	0.033	0.8316
	Cu^{2+}	2.37	7.51	0.9429	1.77	0.32	0.7778	0.021	0.9998	0.053	0.8839
	Cd^{2+}	1.85	22.31	0.9616	1.61	0.20	0.9541	0.004	0.9999	0.020	0.8635
	Sr^{2+}	1.35	2.83	0.9615	0.84	0.28	0.8412	0.053	0.9991	0.177	0.6640
ZTNT3	Pb^{2+}	1.31	63.20	0.9936	1.13	0.19	0.9147	0.002	0.9979	0.026	0.9103
	Cu^{2+}	1.93	7.30	0.9429	1.41	0.30	0.7732	0.008	0.9999	0.027	0.8312
	Cd^{2+}	1.65	29.36	0.9732	1.38	0.24	0.8692	0.008	0.9993	0.025	0.8471
	Sr^{2+}	1.51	2.18	0.9631	0.42	0.42	0.8521	0.004	0.9952	0.046	0.6531
TNT	Pb^{2+}	2.22	24.37	0.9722	1.95	0.26	0.9329	0.288	0.9999	0.052	0.4377
	Cu^{2+}	2.08	7.63	0.9461	1.62	0.26	0.8652	0.192	0.9996	0.068	0.4263
	Cd^{2+}	1.94	21.11	0.9855	1.54	0.30	0.7704	0.116	0.9998	0.029	0.6956
	Sr^{2+}	1.30	6.31	0.9689	0.84	0.27	0.8432	0.069	0.9999	0.031	0.7321

REFERENCES

1 Lagergren, S., *Kungliga Svenska Vetenskapsakademius Hadndlingar*,1898, **24**, 1-39.

2 Freundlich, H., *Trans. Farad. Soc.*, 1932, **28**, 195-201.